Anti-cancer activity and mechanisms of 25-anhydrocimigenol-3-*O*-β-D-xylopyranoside isolated from *Souliea vaginata* on hepatomas

Ze Tian[a,b], Liang Zhou[a], Feng Huang[a,c], Sibao Chen[a,c], Junshan Yang[a], Erxi Wu[d], Peigen Xiao[a] and Mengsu Yang[b]

Our previous study first revealed the cytotoxicity and relative selectivity of 25-anhydrocimigenol-3-*O*-β-D-xylopyranoside (ACX) on HepG2 and R-HepG2 cells. In the present study, the anti-cancer activity and mechanisms of ACX isolated from *S. vaginata* were investigated both *in vitro* and *in vivo*. ACX showed significant, consistent anti-proliferative activity on hepatoma bel-7402 cells by MTT and clone formation assays with an IC_{50} value of 18 μmol/l. Morphological observation and flow cytometry results showed that apoptosis and G_0/G_1 cell cycle arrest contributed to the cytotoxic and cytostatic effects. Further studies showed that Bax and p21 protein expression were upregulated, Bcl-2 protein expression was downregulated, and poly(ADP-ribose) polymerase protein was cleaved. Moreover, ACX also exhibited a dose-dependent inhibition of tumor growth on mice implanted with H_{22} *in vivo*. These findings implicate ACX as a promising anti-cancer agent for chemotherapy of certain cancers. *Anti-Cancer Drugs* 17:545–551 © 2006 Lippincott Williams & Wilkins.

Anti-Cancer Drugs 2006, **17**:545–551

Keywords: 25-anhydrocimigenol-3-*O*-β-D-xylopyranoside, anti-proliferation, apoptosis, cell cycle, implanted mice hepatoma

[a]Institute of Medicinal Plant Development, Chinese Academy of Medical Sciences and Peking Union Medical College, Beijing, China, [b]Department of Biology and Chemistry, City University of Hong Kong, Hong Kong, China, [c]Department of Application of Biology and Chemistry Technology, The Hong Kong Polytechnic University, Hong Kong, China and [d]Children's Hospital Informatics Program at Harvard–MIT Division of Health Sciences and Technology, Children's Hospital Boston, Harvard Medical School, Boston, Massachusetts, USA.

Correspondence to P. Xiao, Institute of Medicinal Plant Development, Chinese Academy of Medical Sciences and Peking Union Medical College, Beijing 100094, China.
Tel: +86 10 6301-1294; fax; +86 10 6303 8753;
e-mail: xiaopg@public.bta.net.cn

Sponsorship: This work is supported by the National Natural Science Foundation of China (30470195 and 30530860), the Area of Excellence Scheme (Institute of Molecular Technology for Drug Discovery and Synthesis) established under the University Grants Committee of the Hong Kong Special Administrative Region, China (AoE/P-10/01), and the National Hi-Tech 863 Program of the Ministry of Science and Technology of China (2003AA2Z2052).

Received 17 November 2005 **Accepted** 26 January 2006

Introduction

Souliea vaginata (Ranunculaceae), an endangered species, is mainly distributed in China. As an anti-inflammatory and analgesic herb, its rhizomes are used to treat conjunctivitis, stomatitis, pharyngitis, enteritis and diarrhea in Chinese folk medicine [1]. Early phytochemical investigations have demonstrated that this species is rich in cycloartane triterpenoids commonly found in plants of the *Cimicifuga* genus [2–6]. Some cycloartane triterpenoids possess potent cytotoxicity. For example, cimicifugoside isolated from *C. simplex* inhibited the proliferation of many cancerous cell lines by blocking the intake of nucleic acids [7]. The compounds 23- or 25-*O*-methoxycimigenol-3-*O*-α-L-arabinopyranoside, actein, cimiracemoside F and cimiracemoside G, isolated from *C. racemosa* showed anti-proliferative activity against HSC-2 cells, with IC_{50} values between 18 and 80 μmol/l, and had less toxicity against normal human gingival fibroblasts [8]. A further study on this species demonstrated that its constituents actein, 23-epi-26-deoxyactein and cimiracemoside A could inhibit growth of MCF-7 human breast cancer cells and induce cell cycle arrest at G_1 by decreasing the level of cyclin D1, cdk4 and the hyperphosphorylated form of the pRb protein, as well as increasing the level of $p21^{Cip1}$ [9]. In addition, three cycloartanes, 23-, 24- and 25-*O*-acetylcimigenol-3-*O*-β-D-xylopyranoside, isolated from *C. dahurica*, were demonstrated to exert their cytotoxicity on HepG2 cells by induction of apoptosis and G_2/M arrest. Downregulation of COX-2 and cdc2 protein expression were involved in the mechanism of apoptosis and G_2/M arrest induced by these three cycloartanes [10]. Our previous study demonstrated the cytotoxicity of 25-anhydrocimigenol-3-*O*-β-D-xylopyranoside (ACX), 25-*O*-acetylcimigenol-3-*O*-β-D-glc(1→2)β-D-xylopyranoside and 25-*O*-acetylcimigenol-3-*O*-β-D-galactopyranoside, isolated from *C. foetida*. These compounds possessed anti-proliferative activity on the HepG2 cell line and its multidrug-resistant cell line R-HepG2, but had relatively low toxicity on primary cultured normal mouse hepatocytes [11]. The underlying mechanism of cytotoxicity of ACX on hepatoma, however, is still unclear. In the current study, the ethanol fraction and chloroform ($CHCl_3$) fraction of *S. vaginata* demonstrated moderate anti-proliferative activity with growth inhibitory activity of 30 and 64% at 200 μg/ml, respectively. ACX was obtained as an active component by

0959-4973

active-directed isolation from the $CHCl_3$ fraction of *S. vaginata*. We investigated the cytotoxicity and mechanisms action on another hepatoma cell line bel-7402, and evaluated its growth inhibitory effect on tumors *in vivo*.

Material and methods

Extraction and isolation

The whole plant of *S. vaginata* (Maxim.) Franch was collected at Qing-Ling Mountain, Gansu Province, China, in August 2002, and identified by Dr Si-bao Chen (Institute of Medicinal Plant Development, Chinese Academy of Medical Sciences and Peking Union Medical College). A voucher specimen (XC-03-0824) was deposited at the same Institute. The air-dried and pulverized whole plant (5.0 kg) was extracted twice with 95% ethanol for 2 h under reflux and then extracted twice with 50% ethanol for another 2 h under reflux. After combination of the ethanol extracts and removal of the solvent, the residue (1.2 kg) was suspended in water and partitioned successively with petroleum ether, $CHCl_3$ and *n*-BuOH. The $CHCl_3$-soluble fraction (400 g) was subjected to low-pressure column chromatography on a silica gel 60H (400–500 mesh) column. Four fractions, A (30 g), B (21 g), C (37 g) and D (60 g), were collected with gradient $CHCl_3$:MeOH (10:0–7:3) solvent elution. Fraction B was further isolated to give a colorless needle (800 mg), melting point 240–242°C. The compound was identified as ACX by comparing the electron ionization mass spectrometry, ^{1}H-NMR and ^{13}C-NMR data with the literature [12]. The purity was more than 95% as determined by HPLC. ACX was dissolved in DMSO at a concentration of 100 mmol/l, then diluted in tissue culture medium and filtered before use.

Cell culture

bel-7402 (from the Institute of Materia Medica, Chinese Academy of Medical Sciences and Peking Union Medical College) cells were maintained in RPMI 1640 (Gibco, Grand Island, New York, USA), containing 10% FBS (Gibco), 2 mg/ml sodium bicarbonate, 100 μg/ml penicillin sodium salt and 100 μg/ml streptomycin sulfate. The cells were grown to 70% confluence, trypsinized with 0.05% trypsin/2 mmol/l EDTA and plated for experimental use.

Cell proliferation assays

Cell proliferation was measured by both MTT and colony formation assays.

bel-7402 (1.5×10^4) cells were seeded in 96-well tissue culture plates and treated with the test compound (100–3.125 μmol/l) or vehicle (0.1% DMSO) at various concentrations and incubated for 48 h followed by the MTT assay at 570 nm [13]. The IC_{50} value was derived from the dose–response curve.

For the colony formation assay, 10^3 bel-7402 cells were plated into six-well, 35-mm diameter culture plates. After 24 h, the cells were treated with different concentrations of the compound or vehicle for 96 h in RPMI 1640 containing 10% FBS. After washing with PBS, colonies were stained with Giemsa solution and then counted. The results were expressed as percentage of the control. A viability of 100% corresponds to the control cells. Each concentration of ACX was tested in triplicate. The relative surviving fraction was plotted on the dose–response curve [14,15].

Morphological study

Cells were cultured in 35-mm culture dishes. After treatment with ACX at 20 μmol/l, all the cultures were incubated at 37°C/5% CO_2 for 48 h. Photographs were taken under an inverted Leica fluorescence 40×10 microscope after acridine orange/ethidium bromide staining [10].

Flow cytometry analysis

bel-7402 cells (1×10^6) were seeded in six-well plates and treated with ACX at 20 μmol/l for 0, 12, 24, 48 and 72 h, respectively. Then, cells were collected and fixed in 70% cold ethanol (−20°C) overnight. After washing twice with PBS, cells were resuspended in PBS containing 1% FCS. RNase A (0.5 mg/ml) and propidium iodide (PI) (2.5 μg/ml) were added to the fixed cells to digest RNA and to stain the cells. The DNA content of cells was then analyzed with a FACSCalibur instrument (Becton Dickinson, San Jose, California, USA) and Coulter (Fullerton, California, USA) Epics XL.

Western blotting

After treatments, cells were washed 3 times with ice-cold PBS and lysed with lysis buffer (50 mmol/l Tris–HCl, pH 7.4, 10 mmol/l EDTA, 1% Triton X-100, 26% urea, and 1 tablet/10 ml protease inhibitor cocktail tablet). Sticky DNA was removed from lysates with a sterile toothpick. The protein concentration of the supernatant was measured by the Bradford method. SDS–PAGE was performed under reducing conditions on 10% polyacrylamide gels and the resolved proteins were transferred onto a nitrocellulose membrane [16,17]. The nitrocellulose membrane was then incubated with mouse anti-human p21 monoclonal antibody (BD Pharmingen, Franklin Lakes, New Jersey, USA), rabbit anti-poly(ADP-ribose) polymerase (PARP) polyclonal antibody (Roche, Nutley, New Jersey, USA), mouse monoclonal anti-Bcl-2 antibody (Santa Cruz Biotechnology, Santa Cruz, California, USA; SC-509) and mouse monoclonal anti-Bax antibody (Santa Cruz; sc-7480). Mouse monoclonal β-actin (Lab Vision, Fremont, California, USA) was used as an internal control. Secondary antibody to IgG conjugated to horseradish peroxidase was used. The blots were detected with ECL according to the manufacturer's instructions.

Fig. 1

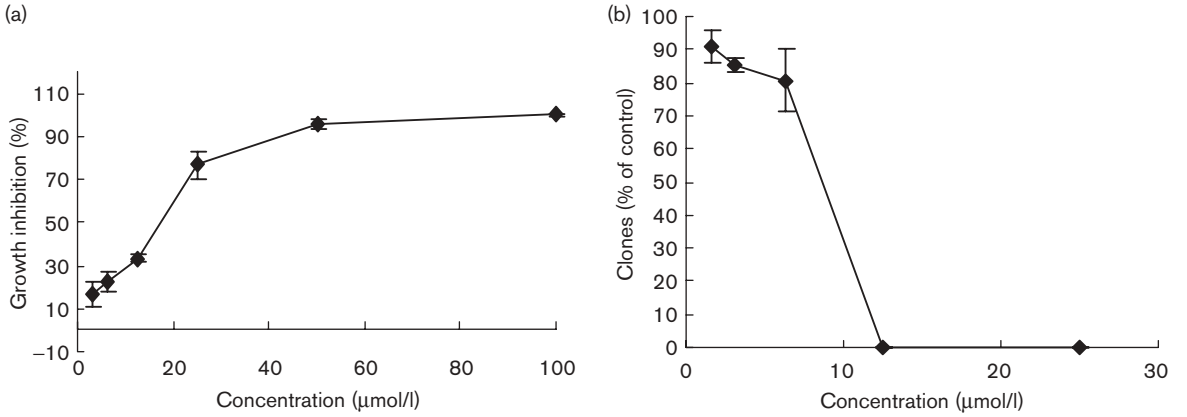

Anti-proliferative activity of ACX on bel-7402 cells. (a) MTT assay of ACX on bel-7402 cells. One of three independent experiments. (b) Clone formation assay of ACX on bel-7402 cells. Means ± SD of three independent experiments.

Anti-cancer evaluation on implanted mouse H_{22}

Male CD-1 (ICR) mice (Beijing Vital Laboratory Animal Technology, Beijing, China), weighing 20–22 g, were used for implantation of hepatoma H_{22} (s.c.), which was maintained by weekly (i.p.) passage in CD-1 (ICR) mice. Ascites (0.2 ml of 1:6 dilution) from tumor-bearing mice 7 days after tumor inoculation were implanted (s.c.) into the armpit region of mice. Eight mice each were treated (i.p.), 24 h after tumor inoculation, with either ACX or vehicle (1% DMSO in saline), once a day for 10 days. Cyclophosphamide (10 mg/kg body weight) was used as a positive control. The tumor inhibition rate (TIR%) was derived from $(1 - T/C) \times 100$, where T is the mean tumor weight of the ACX-treated group and C is the mean tumor weight of the vehicle-treated control group [18].

Statistics

Student's t-test was used and $P < 0.05$ was considered significant.

Results

Anti-proliferative activity of ACX

The in-vitro anti-proliferative activity of the compound on bel-7402 cells was evaluated by MTT and clone formation assays. The results of both MTT and clone formation showed a dose-dependent growth-inhibitory effect (Fig. 1). The IC_{50} value derived directly from concentration–effect curves was about 18 μmol/l. In the clone formation assay, there was no clone formed at the end of the time tested with higher concentrations (25 μmol/l). With 12.5 μmol/l, there were some small clones formed, but the clone numbers and cell numbers in a clone (all below 50) were fewer than that of vehicle control. At 6.25 μmol/l, some clones were small, but cell numbers in a clone were above 50. This indicated that both cytotoxic and cytostatic effects were involved in the anti-proliferation of the compound. With higher concentrations, it mainly showed cytotoxic effects; with lower concentrations, it showed cytostatic effects.

Apoptosis morphological alteration induced by ACX

The fluorescence staining method was introduced to investigate individual apoptosis in the cell population treated by ACX. After treatment at 20 μmol/l for 48 and 72 h, morphological changes of the cells were significant. Chromatin aggregation, nuclear and cytoplasmic condensation, and partition of cytoplasm and nucleus into membrane-bound vesicles (apoptotic bodies) were observed (Fig. 2)

Effect of ACX on cell cycle progression

To elucidate the cytostatic effect of ACX on bel-7402 cells, specific cell cycle progression was determined by flow cytometry. After exposure to ACX at a concentration of 20 μmol/l for 0, 12, 24, 48 and 72 h, cell cycle progression of bel-7402 cells changed significantly in comparison with the control (Fig. 3). It caused significant G_0/G_1 arrest with a concomitant decrease of the cell population in S phase and a small sub-G_1 peak, which was recognized as the apoptotic fraction at 48 and 72 h.

Regulation of apoptosis and cell cycle-related protein expression

PARP is an early hallmark of apoptosis and is used to further confirm the apoptosis event in cell populations treated with cytotoxic agents. For treatment with 20 μmol/l ACX, 113-kDa PARP protein began to be cleaved into 89- and 24-kDa fragments at the 12-h time point and continued in a time-dependent manner. This indicated that activation of caspases was involved in apoptosis of bel-7402 cells. Furthermore, treatment

Fig. 2

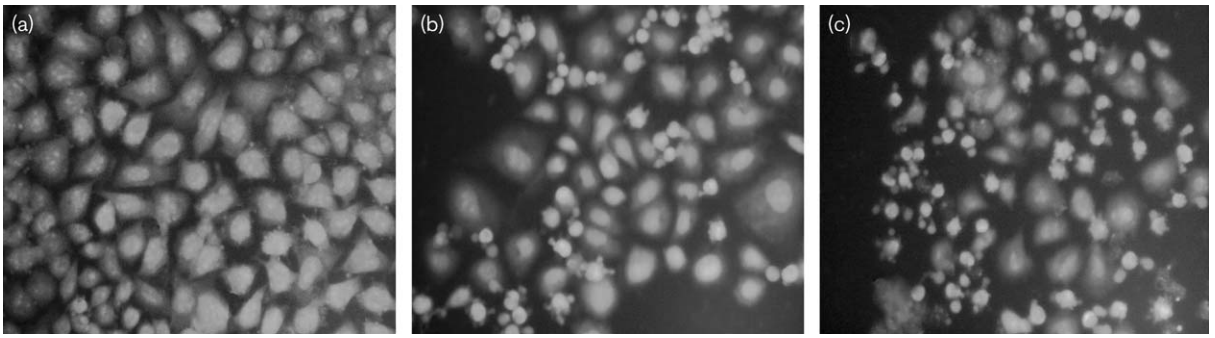

Morphological changes of apoptosis on bel-7402 cells in response to ACX. Cells were stained by acridine orange/ethidium bromide and observed under an inverted Leica fluorescence 40 × 10 microscope: (a) control; (b and c) treatment with ACX at 20 μmol/l for 48 and 72 h, respectively.

Fig. 3

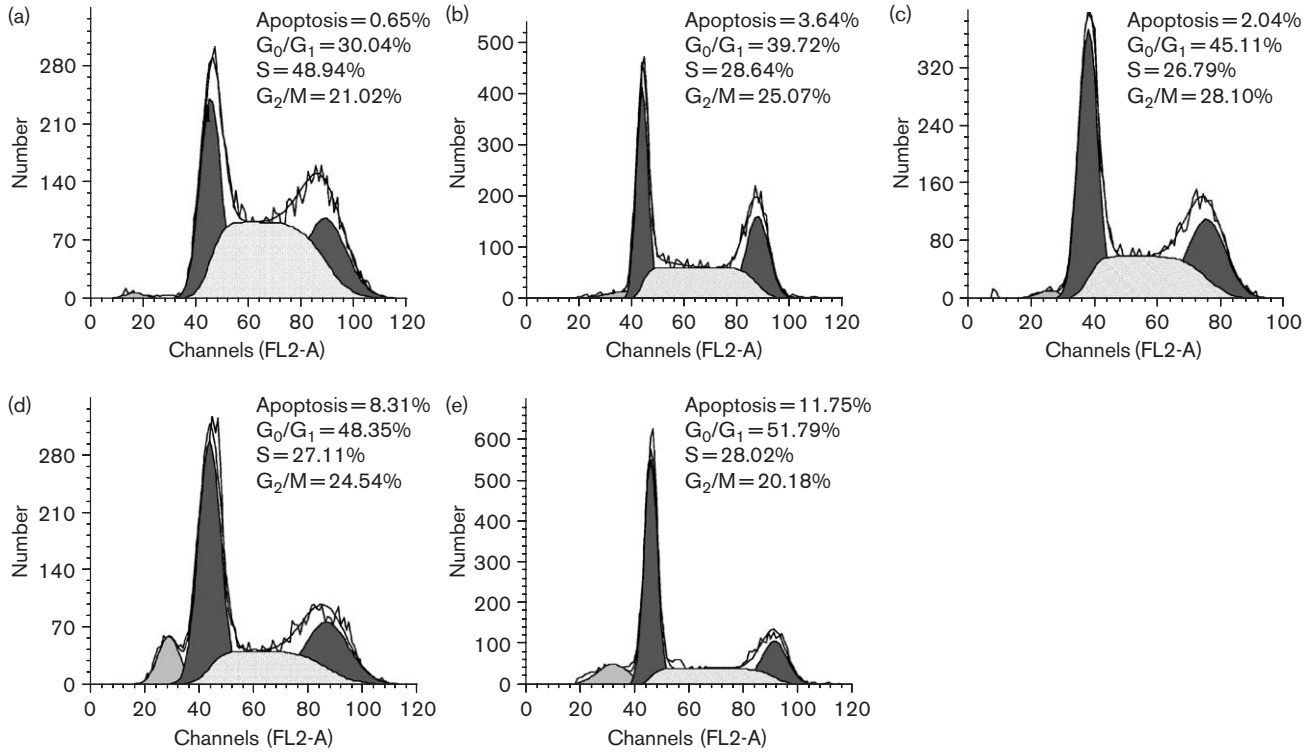

Cell cycle distribution of bel-7402 cells treated with ACX. Cells were stained with PI and analyzed by flow cytometry: (a) bel-7402 control; (b–e) bel-7402 cells treated with ACX at 20 μmol/l for 12, 24, 48 and 72 h. The results shown here were from one of three representative experiments.

with the compound at 20 μmol/l could upregulate the expression of the pro-apoptotic protein Bax and down-regulate the anti-apoptotic protein Bcl-2 in a time dependent manner (Fig. 4). p21 is a cyclin-dependent kinase (CDK) inhibitor (CKI) that plays a key role in apoptosis and G_1 to S cell cycle progression. Treatment with ACX at 20 μmol/l could significantly induce the expression of p21 protein in bel-7402 cells (Fig. 4).

Inhibition of tumor growth by ACX

After tumor implantation for 24 h (i.p.), treatment with ACX (30, 15 or 7.5 mg/kg body weight) or cyclophosphamide (10 mg/kg body weight) once a day for 10 days could significantly suppress the growth of H_{22} (Table 1). Meanwhile, significant body weight loss was observed in the cyclophosphamide-treated group compared with that of the control, whereas only slight body weight loss was

Fig. 4

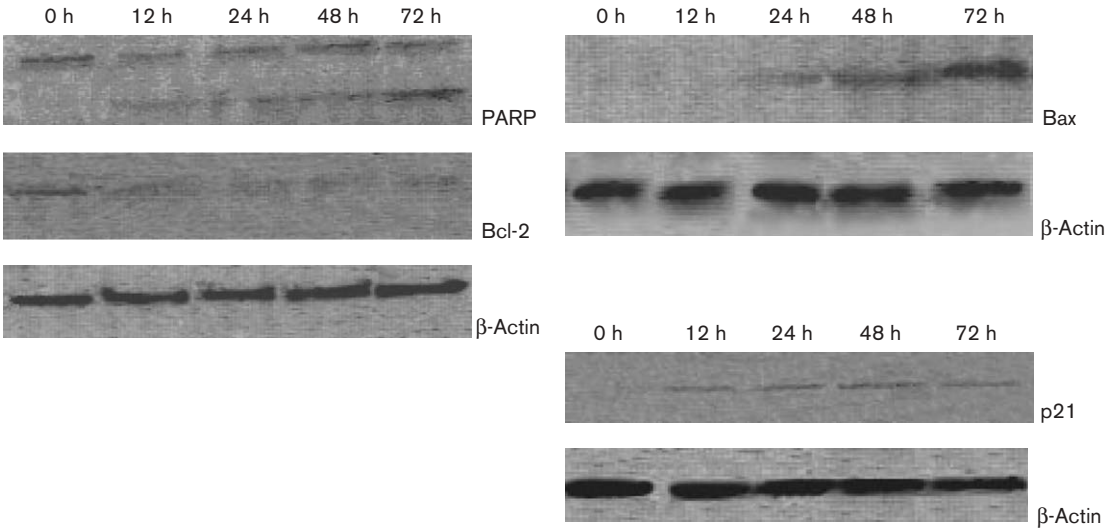

Regulation of apoptosis and cell cycle-related protein expression on bel-7402 cells treated by ACX. Cellular lysate protein (50 μg/lane) was loaded on a 10% SDS–polyacrylamide gel, electrophoresed and subsequently transferred onto nitrocellulose membranes. Immunoblots were probed with antibodies specific for PARP, Bcl-2, Bax and p21. Lysates were from bel-7402 cells treated with 20 μmol/l ACX for 0, 12, 24, 48 and 72 h, respectively.

Table 1 Tumor growth inhibitory effect of ACX on H_{22}

Samples	Dosage (mg/kg)	Tumor weight (g)	Tumor growth inhibition (%)
Control	–	2.87 ± 1.38	–
Cyclophosphamide	10	1.18 ± 0.45[b]	58.89
ACX	30	1.41 ± 0.88[a]	50.87
ACX	15	1.66 ± 0.73[a]	42.16
ACX	7.5	1.72 ± 0.72[a]	40.07

[a]$P<0.05$ and [b]$P<0.01$ compared with control.

observed in the ACX-treated group. This implied that ACX might possess an anti-hepatoma effect *in vivo* with low toxicity.

Discussion

Hepatoma (hepatocellular carcinoma) is a relatively common malignancy, ranking fifth in frequency on a worldwide basis and causing more than 1 million deaths annually [14]. Moreover, one-third of Asian hepatoma cases occur in China [19] and the incidence has been continually increasing in recent years. There is still no effective chemotherapy for this disease at present.

ACX was of considerable interest because it has shown selective cytotoxicity to hepatoma HepG2 cells, but has shown less cytotoxicity on primary cultured normal mouse hepatocytes, as described in our previous study. In this paper, we first showed anti-proliferative activity of ACX on another hepatoma, bel-7402 cells, and demonstrated that apoptosis and G_0/G_1 cell cycle arrest were involved in the cytotoxic and cytostatic effect, respectively.

Many anti-cancer agents arrest the cell cycle at the G_1, S or G_2/M phase and then induce apoptotic cell death [20–22]. The death receptor pathway and the mitochondrial pathway are the two major routes that have been identified to be associated with drug-induced apoptosis. In particular, the Bcl-2 protein family plays a central role in the regulation of the mitochondrial apoptosis pathway. Members of Bcl-2 family proteins can be divided into two subfamilies: the anti-apoptotic proteins such as Bcl-2 and Bcl-X_L, and the pro-apoptotic proteins such as Bax, Bad and Bid. The family members, e.g. Bcl-2 and Bax, form homodimers and heterodimers; the ratio between these dimers is, in turn, crucial to modulate the apoptotic response. The overexpression of Bcl-2 has been shown to block the release of cytochrome *c* in response to a variety of apoptotic signals. On the contrary, the Bax protein promotes cytochrome *c* release from the mitochondria. Released cytochrome *c* activates caspase-9 to initiate the caspase cascades, followed by proteolytic executioner caspase-3, which catalyzes proteolysis of many different substrates, such as DNA repair proteins, cell cycle regulatory proteins, and components of the nucleus and cytoskeleton [23–28]. The 113-kDa PARP, a nuclear enzyme that specifically binds to damaged DNA, is a substrate of an apoptotic-specific protease from caspases, and is cleaved during apoptosis into 89- and 24-kDa fragments, which could serve as an early hallmark of apoptosis [29]. In the present study, we have shown that ACX treatment of bel-7402 cells leads to a significant increase in the level of the pro-apoptotic Bax protein and decrease in the level of the anti-apoptotic Bcl-2 protein. Thus, alteration of the Bax/Bcl-2 ratio was of benefit to

apoptosis. Furthermore, PARP protein was cleaved in our investigation. It appears that the apoptosis of bel-7402 cells induced by ACX might be through the mitochondrial pathway, and regulation of Bax/Bcl-2 protein expression and activation of caspases is associated with this process. The cell cycle is tightly governed by sequential CDKs, which are activated by cyclins, whose expression is regulated throughout the cell cycle. The activity of cyclin/CDK complexes is, in turn, negatively regulated by a number of CKIs [30–32]. p21 belongs to one of two distinct CKI families, i.e. the Cip/Kip family. It could arrest cell cycle progression at the G_1 phase by suppressing the activity of most CDKs and binding to the proliferating cell nuclear antigen, which is a cofactor of DNA polymerase δ, to inhibit the synthesis of DNA directly [33,34]. In our study, p21 protein expression was increased significantly in a time-dependent manner. This implies that the upregulation of p21 may contribute to G_0/G_1 arrest on bel-7402 cells treated by ACX.

It is well known that there is a certain correlation between the results of in-vitro and in-vivo studies. Although the effective compounds *in vitro* might have less or no effect *in vivo*, the cytotoxicity *in vitro* against cancer cell lines from a particular organ would predict cytotoxicity against corresponding tumors in animals and humans. Fortunately, our results showed that ACX inhibited tumor growth of mice bearing hepatoma H_{22} without evident body weight loss in a dose-dependent manner. This predicts that ACX may inhibit corresponding hepatoma growth in humans with low toxicity.

In conclusion, ACX possesses anti-hepatoma activity both *in vitro* and *in vivo*. It exerts its anti-proliferative activity via apoptosis and G_0/G_1 cell cycle arrest, through the regulation of Bcl-2/Bax and activation of caspases. The results reported herein may suggest the potential clinical application of ACX on hepatoma treatment in the future.

Acknowledgments

We thank Annie Moseman for thoughtful reading of the manuscript.

References

1 Institute of Botany, Chinese Academy of Sciences and Institute of Materia Medica, Chinese Academy of Medical Sciences. *Flora Republicae Popularis Sinicae 27*. Beijing: Science Press; 1979. pp. 91–93.
2 Zhou L, Yang JS, Zou JH, Tu GZ. Three new cycloartane triterpene glycosides from *Souliea vaginata*. *Chem Pharm Bull* (Tokyo) 2004; **52**: 622–624.
3 Zhou L, Yang JS, Wu X, Zou JH, Xu XD, Tu GZ. Two new cycloartane triterpene glycosides and a new alkaloid from *Souliea vaginata*. *Heterocycles* 2005; **65**:1409–1414.
4 Zhou L, Yang JS, Tu GZ. A new cycloartane triterpene glycoside from *Souliea vaginata*. *Chin Chem Lett* 2005; **16**:1047–1049.
5 Pan RL, Chen DH, Si JY, Zhao XH, Shen LG. Studies on the triterpenoid constituents from the aerial part of *Cimicifuga foetida*. *Acta Pharm Sinica* 2002; **37**:117–120.
6 Liu Y, Chen DH, Si JY, Pan RL, Tu GZ, An DG. Two new cyclolanstanol xylosides from the aerial parts of *Cimicifuga dahurica*. *J Nat Prod* 2002; **65**:1486–1488.
7 Kusano G. Studies on the constituents of *Cimicifuga* species. *Yakugaku Zasshi* 2001; **121**:497–521.
8 Watanabe K, Mimaki Y, Sakagami H, Sashida Y. Cycloartane glycosides from the rhizomes of *Cimicifuga racemosa* and their cytotoxic activities. *Chem Pharm Bull* 2002; **50**:121–125.
9 Einbond LS, Shimizu M, Xiao D, Nuntanakorn P, Lim JT, Suzui M, *et al.* Growth inhibitory activity of extracts and purified components of black cohosh on human breast cancer cells. *Breast Cancer Res Treat* 2004; **83**:221–231.
10 Tian Z, Yang MS, Huang F, Li KG, Shi L, Chen SB, *et al.* Cytotoxicity of three cycloartane triterpenoids from *Cimicifuga dahurica*. *Cancer Lett* 2005; **226**:65–75.
11 Tian Z, Pan RL, Si JY, Xiao PG. Cytotoxicity of cycloartane triterpenoids from aerial part of *Cimicifuga foetida*. *Fitoterapia* 2006; **77**:39–42.
12 Kadota S, Li JX, Tanaka K, Namba T. Constituents of *Cimicifuga*e rhizome. Isolation and structures of new cycloartenol triterpenoids and related compounds from *Cimicifuga foetida* L. *Tetrahedron* 1995; **51**:1143–1166.
13 Carmichael J, DeGraff WC, Gazdar AF, Minna JB, Mitchell JB. Evaluation of a tetrazolium-based semiautomated colorimetric assay: assessment of chemosensitivity. *Cancer Res* 1987; **47**:936–942.
14 Suzui M, Masuda M, Lim J, Albanese C, Pestell RG, Weinstein IB. Growth inhibition of human hepatoma cells by acyclic retinoid is associated with induction of $p21^{CIP1}$ and inhibition of expression of cyclin D11. *Cancer Res* 2002; **62**:3997–4006.
15 Shimizu M, Suzui M, Deguch A, Lim JT, Xiao D, Hayes JH, *et al.* Synergistic effects of acyclic retinoid and OSI-461 on growth inhibition and gene expression in human hepatoma cells. *Clin Cancer Res* 2004; **10**:6710–6721.
16 Laemmli UK. Cleavage of structural proteins during the assembly of the head of bacteriophage T4. *Nature* 1970; **227**:680–685.
17 Towbin H, Staehelin T, Gordon J, Electrophoretic transfer of proteins from polyacrylamide gels to nitrocellulose sheets: procedure and some applications. *Proc Natl Acad Sci U S A* 1979; **76**:4350–4354.
18 Kumara SS, Hauat BT. Extraction, isolation and characterization of antitumor principle, α-hederin, from the seeds of *Nigella sativa*. *Planta Med* 2001; **67**:29–32.
19 Yeh CT, Yen GC. Induction of apoptosis by the anthocyanidins through regulation of Bcl-2 gene and activation of c-Jun N-terminal kinase cascade in hepatoma cells. *J Agric Food Chem* 2005; **53**:1740–1749.
20 Piao W, Yoo J, Lee DK, Hwang HJ, Kim JH. Induction of G_2/M phase arrest and apoptosis by a new synthetic anti-cancer agent, DW2282, in promyelocytic leukemia (HL-60) cells. *Biochem Pharmacol* 2001; **62**: 1439–1447.
21 Kessel D, Luo Y. Cells in cryptophycin-induced cell-cycle arrest are susceptible to apoptosis. *Cancer Lett* 2000; **151**:25–29.
22 Fujimoto K, Hosotani R, Doi R, Wada M, Lee JU, Koshiba T, *et al.* Induction of cell cycle arrest and apoptosis by a novel retinobenzoic-acid derivative, TAC-101, in human pancreatic-cancer cells. *Int J Cancer* 1999; **81**: 637–644.
23 Tong X, Lin S, Fujii M, Hou DX. Molecular mechanisms of echinocystic acid-induced apoptosis in HepG2 cells. *Biochem Biophys Res Commun* 2004; **321**:539–546.
24 Oh SH, Lee BH. A ginseng saponin metabolite-induced apoptosis in HepG2 cells involves a mitochondria-mediated pathway and its downstream caspase-8 activation and Bid cleavage. *Toxicol Appl Pharmacol* 2004; **194**:221–229.
25 Changa JS, Hsub YL, Kuo P, Kuo Y, Chiang L, Lin C. Increase of Bax/Bcl-X_L ratio and arrest of cell cycle by luteolin in immortalized human hepatoma cell line. *Life Sci* 2005; **76**:1883–1893.
26 Ocker M, Herold C, Ganslmayer M, Zopf S, Hahn EG, Schuppan D. Potentiated anticancer effects on hepatoma cells by the retinoid adapalene. *Cancer Lett* 2004; **208**:51–58.
27 Thornberry NA, Lazebnik Y. Caspases: enemies within. *Science* 1998; **281**:1312–1316.
28 Sane AT, Bertrand R. Caspase inhibition in camptothecin-treated U-937 cells is coupled with a shift from apoptosis to transient G_1 arrest followed by necrotic cell death. *Cancer Res.* 1999; **59**:3565–3569.
29 Zhang MC, Liu HP, Demchik LL, Zhai YF, Yang da J. Light sensitizes IFN-gamma-mediated apoptosis of HT-29 human carcinoma cells through both death receptor and mitochondria pathways. *Cell Res* 2004; **14**:117–124.
30 Buecher B, Broquet A, Bouancheau D, Heymann MF, Jany A, Denis MG, *et al.* Molecular mechanisms involved in the antiproliferative effect of two COX-2 inhibitors, nimesulide and NS-398, on colorectal cancer cell lines. *Dig Liver Dis* 2003; **35**:557–565.

31 Niculescu AB, Chen X, Smeets M, Hengst L, Prives C, Reed SI. Effects of $p21^{Cip1/Waf1}$ at both the G_1/S and the G_2/M cell cycle transitions: pRb is a critical determinant in blocking DNA replication and in preventing endoreduplication. *Mol Cell Biol* 1998; **18**:629–643.
32 Nakanishi M, Kagawa Y, Takahashi H, Matsushime H. Two different bindings of p21 Cdk inhibitor to cyclin/Cdk complex. *Leukemia* 1997; **11** (**Suppl**):356–357.
33 Coleman ML, Marshall CJ, Olson MF. Ras promotes $p21^{Waf1/Cip1}$ protein stability via a cyclin D1-imposed block in proteasome-mediated degradation. *EMBO J* 2003; **22**:2036–2046.
34 Garcia-Wilson E, Perkins ND. $p21^{WAF1/CIP1}$ regulates the p300 HSumoylation motif CRD1 through a C-terminal domain independently of cyclin/CDK binding. *Cell Cycle* 2005; **4**: 1113–1119.